Desalination and Water Treatment
www.deswater.com
doi: 10.1080/19443994.2015.1012746

57 (2016) 6809–6819
March

Taylor & Francis
Taylor & Francis Group

Application of dendrimer/titania nanohybrid for the removal of phenol from contaminated wastewater

Bagher Hayati[a], Mokhtar Arami[b,*], Afshin Maleki[a], Elmira Pajootan[b]

[a]*Kurdistan Environmental Health Research Center, Kurdistan University of Medical Sciences, Sanandaj, Iran, emails: bagherhayati90@gmail.com (B. Hayati), malaki@oa.muk.ac.ir (A. Maleki)*
[b]*Textile Engineering Department, Amirkabir University of Technology, Tehran, Iran, Tel. +98 21 64542614; Fax: +98 21 66400245; emails: arami@aut.ac.ir (M. Arami), pajootan@aut.ac.ir (E. Pajootan)*

Received 20 July 2014; Accepted 14 January 2015

ABSTRACT

In this study, polyamidoamine dendrimer of generation 4 was successfully immobilized on titania nanoparticles to synthesize a new nanohybrid (Den/TiO_2) with the capability of encapsulation for phenol removal from the polluted effluents. Characterizations of the adsorbent using SEM, TEM, XRD, and FTIR analyses indicated the successful immobilization of dendrimers onto the surface of titania. The effect of important parameters on removal efficiency such as retention time, pH, phenol concentration, Den/TiO_2 dosage, and temperature was investigated. The isotherm, kinetic, and thermodynamic parameters of the removal process were demonstrated, and the experimental data followed the Langmuir and pseudo-second-order model with high correlation coefficients. The calculated thermodynamic parameters showed that the removal of phenol using Den/TiO_2 was an endothermic and spontaneous process. The obtained results indicate that the prepared nanohybrid can be effectively used for the removal of phenol from industrial wastewaters.

Keywords: Den/TiO_2 nanohybrid; Phenol removal; Isotherm; Kinetic; Thermodynamic

1. Introduction

Phenol intoxication even at relatively low concentrations is a serious environmental threat due to the carcinogenic and toxic nature of this organic compound [1,2]. The major sources of phenol introduction into the environment are industrial processes. Various removal methods such as membrane processes (dialysis, electrodialysis, reverse osmosis, etc.), neutralization precipitation, extraction, and adsorption have been extensively employed for the removal of phenol from contaminated effluents [3]. However, the development of more economical alternatives remains a major goal. The encapsulation is one of the low-cost and environmentally friendly techniques which has the potential to overcome the limitations of other removal strategies especially adsorption processes using polymers, activated carbon, and natural adsorbents [4,5].

Recently, high surface area materials particularly dendrimers, are appealing for the separation applications [6]. Dendrimers are hyperbranched molecules composed of monomers, which radiate from a central core. These molecules are recently emerging as an important class of polymers and their physical and

*Corresponding author.

chemical properties are affected by their structure. Dendrimers of higher generations have a close-packed spherical periphery surrounding the interior cavities which will cause crowding of the surface functional groups [7]. The unique behavior of dendrimer molecules makes them suitable for a wide range of applications including environmental remediation, nanoparticle synthesis, and nanomedicine [8–10]. Polyamidoamine (PAMAM) is among the least toxic and most studied dendrimers which is made of readily available materials [11]. In general, dendrimers have attracted attention because of their well-defined structures and chemical versatility.

However, the commercial applications of these materials have not been well explored. Initial efforts in the application of PAMAM dendrimers have been focused on their early generations having the flat ellipsoidal shape [12–14]. On the other hand, dendrimers of higher generations (generation 4 and above) are starburst shaped and are particularly appealing to modern applications. One of the specific properties of PAMAM dendrimer is their ability to encapsulate organic compounds like phenol to remove from solutions. This attribution has been primarily exploited in the synthesis of metal nanoparticles; and dendrimer-based encapsulation or dendrimer-based hybrids (nanohybrids) have gained great interests [9,15–20].

In the present study, PAMAM dendrimers with ethylenediamine cores of generation 4 (G_4-NH_2) were immobilized on the surface of titania (TiO_2) nanoparticles to synthesize a new nanohybrid material (Den/TiO_2). The properties of the prepared adsorbent were investigated for the encapsulation of phenol molecules. The synthesis of the new inorganic/organic nanohybrid is based on the popularity of the amine-terminated PAMAM dendrimer for the environmental applications. On the other hand, titania nanoparticles with high thermal and chemical stability are selected for the initial effort of making a novel nanohybrid material to combine the extraordinary properties of both materials, such as their nanodimensions, and non-toxic nature. The immobilization and retention of dendrimer on titania was demonstrated by scanning electron microscope (SEM), transmission electron microscope (TEM), X-ray diffraction (XRD), and Fourier transform infrared (FTIR) analysis; and the newly synthesized Den/TiO_2 was used as a novel adsorbent for the removal of phenol from synthetic solutions. The main advantage of TiO_2 nanoparticles was the occupation of the terminated amino groups of PAMAM to exclude the repulsion forces between the phenol molecules and dendrimer surface groups. Critical parameters that influence the removal efficiency including pH, time, phenol concentration, and adsorbent dosage have been investigated. The isotherm, kinetic, and thermodynamic parameters have also been studied in this research.

2. Materials and methods

2.1. Materials

Generation 4 PAMAM dendrimer (G_4-NH_2) was purchased from Sigma Aldrich (10% (w:w)) with methanol as the solvent and it was used without further purification. The diameter of dendrimer molecules was 4.5 nm with ethylenediamine as the core (2-carbon core) containing 64 external amino functional groups. Its overall formula is shown in Table 1. Titanium(IV) dioxide (TiO_2) (99.5% purity, 50–100 nm particle size) was purchased from Merck. All the other reagents were of analytical grade and were supplied from Sigma Aldrich or Merck.

2.2. Synthesis and characterization of Den/TiO_2 nanohybrid

The first step of the simple and economical synthesis of Den/TiO_2 nanohybrid was the dilution of the G_4-NH_2 PAMAM-methanol solution (1 g) in a large amount of deionized water. TiO_2 nanoparticles were slowly added to the diluted dendrimer solution to achieve a slurry mixture (1:99 (w:w)). The solution was sonicated (VWR ultrasonic cleaner, 150 W, 50 kHz) for 120 min, and the Den/TiO_2 material was then dried on a hot plate ($T = 60$ °C) and drying oven ($T = 90$ °C) to remove the solvent and excess moisture, respectively [21].

2.3. Characterization of Den/TiO_2

FTIR spectra of TiO_2, PAMAM, and the prepared Den/TiO_2 were obtained by employing a Perkin-Elmer Spectrophotometer Spectrum One within the range of 350–4,000 cm^{-1}.

XRD of TiO_2 and Den/TiO_2 was performed using a Philips powder diffractometer PW 1800.

TEM and SEM were also employed to analyze the morphology of TiO_2 and Den/TiO_2.

Table 1
Formula and properties of PAMAM dendrimer (G_4)

Generation	Molecular weight (g/mol)	Measured diameter (nm)	Surface groups
4	14,215	45	64

2.4. Phenol removal process

The removal of phenol was carried out in 100 mL conical flask by the combination of the appropriate amount of phenol and Den/TiO_2 nanohybrid. The solution was mixed using a magnetic stirrer at 200 rpm. The pH of the aqueous solutions was adjusted from 3 to 9 using HCl (1 M) or NaOH (1 M) monitored by a pH meter. Experiments were conducted for 90 min. The samples were taken from the solution at various time intervals and they were centrifuged at 7,000 rpm for 10 min. The phenol concentrations were analyzed by spectroscopy measurements according to ASTM D1783-01 method using 4-aminoantipyrine (20.8 mM in 0.25 mM $NaHCO_3$) and potassium ferricyanide (83.4 mM $K_3Fe(CN)_6$ in 0.25 mM $NaHCO_3$). Phenol reacts with 4-aminoantipyrine under the alkaline condition and it will be oxidized in the presence of potassium ferricyanide reagent. The obtained quinone-type dye compound absorbs light at 510 nm [22]. The efficiency of phenol removal was calculated using Eq. (1):

$$\% \text{ Phenol removal efficiency} = (C_0 - C)/C_0 \times 100 \quad (1)$$

where C_0 and C are the initial and retained phenol concentration, respectively.

Adsorption isotherm indicates the relation between the mass of phenol adsorbed at a constant temperature per unit mass of the adsorbent and phenol concentration in liquid phase at equilibrium. In addition, it shows how phenol molecules can be distributed between the liquid and solid phases at various equilibrium concentrations, and how efficiently a given adsorbent interacts with the adsorbate. Several factors such as the number of compounds in the solution, their relative adsorbabilities, initial concentration of adsorbate in the solution, and the degree of competition among the solutes for the adsorption sites determine the shape of the isotherm [23]. In this research, the Langmuir and Freundlich isotherms have been surveyed.

The pseudo-first- and pseudo-second-order kinetic models have been investigated for the removal of phenol from contaminated solutions. Kinetic data provide information (such as the adsorbate residence time and reactor dimension) about the mechanism of a process. It is important to know the rate of the adsorption during the removal of contaminants from wastewater in order to optimize the design parameters and to achieve high efficiencies. As a result, predicting the removal rate for a given system is probably the most important factor to design an adsorption system [24].

3. Results and discussion

3.1. Characterization of Den/TiO_2

3.1.1. FTIR spectra

The immobilization of dendrimer onto titania nanoparticles was verified by FTIR analysis. Fig. 1 shows the FTIR spectra of pure TiO_2, PAMAM dendrimer, and Den/TiO_2. The peaks at 2,972 and 2,855 cm^{-1} are corresponding to C–H stretching bond. The peaks appearing at 1,648, 1,279, and 1,546 cm^{-1} indicate the amide functionality through C=O stretching, C–N stretching, and amide C–N–H bending/closing or bending/opening, respectively. The corresponding peaks at 1,459, 1,428, and 1,349 cm^{-1} associate, respectively, with the H–C–H scissoring, H–C–H asymmetric deformation, and H–C–H rocking, wagging, and twisting (Fig. 1(b)).

These appeared peaks for PAMAM dendrimer also exist in the FTIR spectra of the synthesized Den/TiO_2 (Fig. 1(c)). In addition, the peak at 1,092 cm^{-1} can be attributed to the Ti–O–C bond, which confirms the chemical interaction between the dendrimer and titania nanoparticles. Similar to TiO_2 nanoparticles

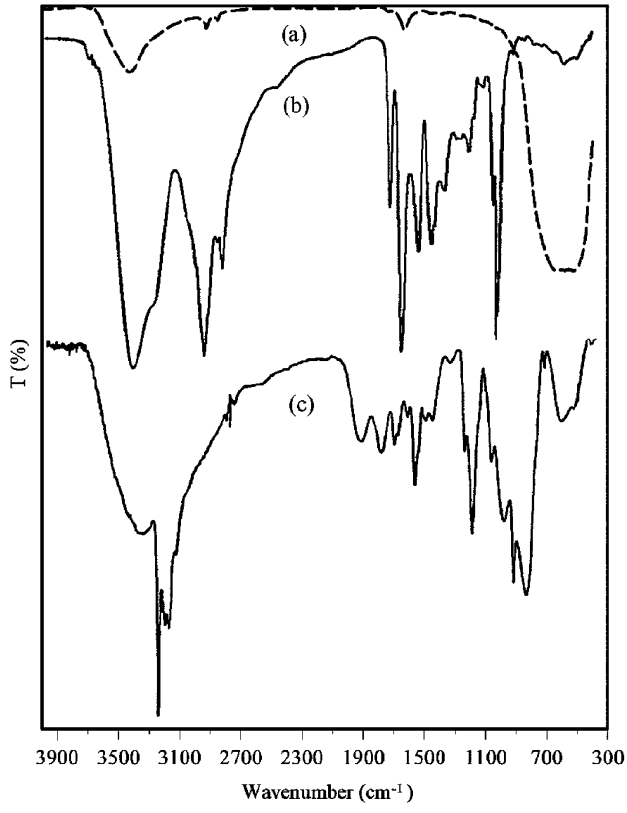

Fig. 1. FTIR patterns of (a) TiO_2 nanoparticles, (b) PAMAM dendrimer, and (c) Den/TiO_2.

(Fig. 1(a)), the broad peak in the range of 500–700 cm^{-1} related to the Ti–O–Ti stretching bond is appeared in Den/TiO_2 too.

Moreover, electrostatic interactions and hydrogen bonding can also be possible for the dendrimer adsorption onto titania. The loading process of PAMAM onto TiO_2 was performed in a solution of pH 7, and since the isoelectric pH (point of zero charge) of titania is 4, the surface of titania was negatively charged unlike the positively charged PAMAM dendrimers. Therefore, a strong electrostatic interaction exists between the dendrimer molecules and TiO_2 nanoparticles. Moreover, PAMAM dendrimers are terminated with 64 amino groups which can form multiple hydrogen bonds with the adsorbed hydroxyl groups on the surface of titania in water [21].

3.1.2. XRD analysis

Fig. 2 shows the XRD patterns of TiO_2 and Den/TiO_2. The peaks corresponding to the anatase TiO_2 phase appeared at $2\theta = 24.9^\circ$, 37.4°, and 47.5°. It is evident that the major phase of the synthesized Den/TiO_2 is predominantly anatase. High intensity of TiO_2 peak is the evidence of the availability of TiO_2 compound. The existence of rutile (27.5°) peaks is also evident. Changes in the pattern of the new Den/TiO_2 between $2\theta = 18.00^\circ$ and 40.00° indicates the intercalation of dendrimer in comparison with the XRD pattern of TiO_2. Also, the significant decrease in the intensity and a slight shifts at $2\theta = 21^\circ$, 23°, 26.66°, and 35.34°, were observed as broadening in the Den/TiO_2 pattern, which are also attributable to the delamination and disorientation of dendrimer structure [25].

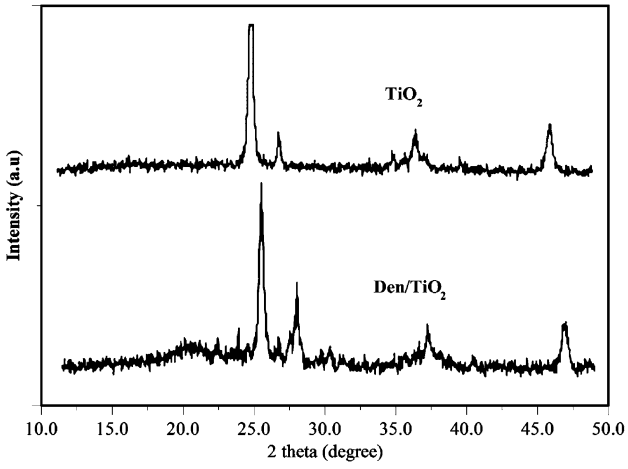

Fig. 2. XRD patterns of TiO_2 and Den/TiO_2.

3.1.3. SEM and TEM images

SEM and TEM images of TiO_2 and Den/TiO_2 are shown in Fig. 3. SEM images show the spherical and porous surfaces of TiO_2 and Den/TiO_2 (Fig. 3(a) and (b)). According to these images, TiO_2 nanoparticles exhibited more aggregation rather than the synthesized Den/TiO_2. This can be confirmed by TEM images of both TiO_2 (Fig. 3(c)) and Den/TiO_2 (Fig. 3(d)). More adherence of TiO_2 nanoparticles are observed in TEM images rather than Den/TiO_2, which displays the dispersion of TiO_2 nanoparticles in the structure of Den/TiO_2. The lower levels of aggregation in the Den/TiO_2 are expected to improve the adsorption properties [26]. Therefore, the combined results of FTIR, XRD, SEM, and TEM analysis confirm the immobilization of TiO_2 nanoparticles on the surface of PAMAM dendrimer.

3.2. Effect of operating parameters

3.2.1. Effect of pH

The effect of pH on the adsorption capability of Den/TiO_2 was investigated. According to Fig. 4, varying the pH of solution do not affect the removal efficiency significantly. This can be explained by the possible electrostatic interactions between the positively charged dendrimer and negatively charged titania, and also by the formation of multiple hydrogen bonds between the adsorbed hydroxyl groups on the surface of titania and terminal amino groups of PAMAM. These interactions could occupy the terminated amino groups of PAMAM and prevent them from interacting with phenol molecules at different pH values. Therefore, the suggested mechanism for the removal of phenol is the encapsulation of phenol molecules in the internal cavities of dendrimer and Van der Waals attraction between the aromatic benzene ring and alkane chains in the structure of PAMAM dendrimer.

On the other hand, if the removal mechanism was on the basis of the electrostatic interactions between the Den/TiO_2 and phenol molecules, the removal efficiencies would be very low, because the surface charge of both adsorbent and adsorbate at various pH values are the same. Therefore, the neutral pH (pH 7) was chosen as the optimum pH value for the subsequent experiments.

3.2.2. Effect of Den/TiO_2 dosage

Fig. 5 represents the effect of adsorbent dosage on the removal of phenol using Den/TiO_2. As shown in

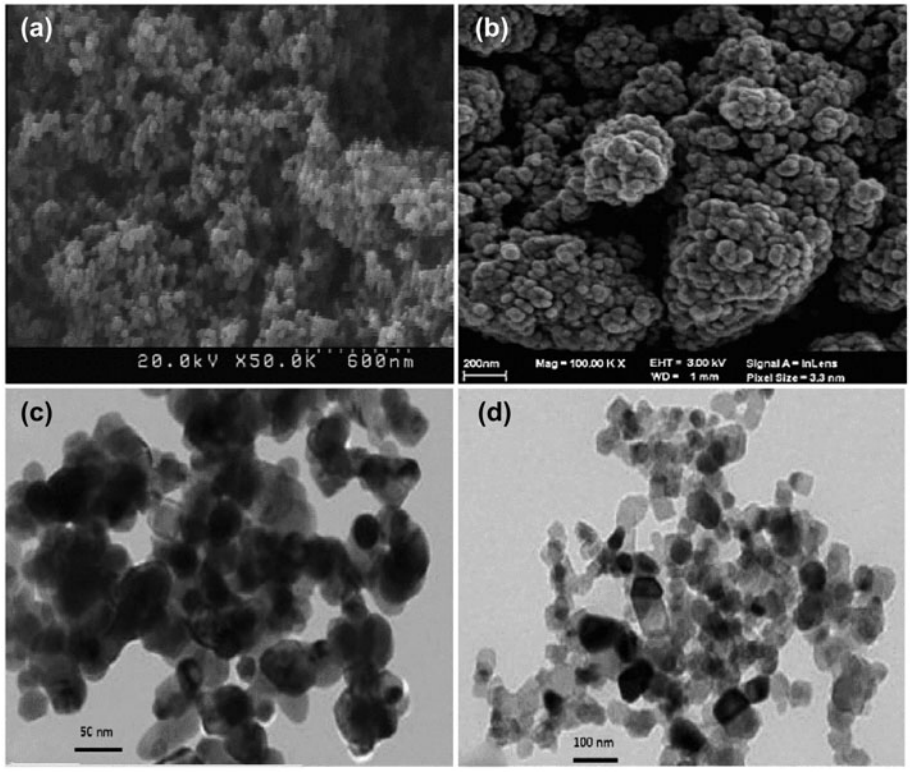

Fig. 3. SEM and TEM images of (a, c) TiO_2 and (b, d) Den/TiO_2.

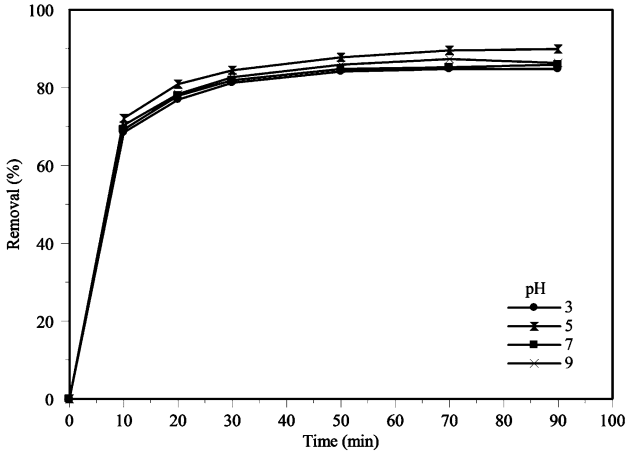

Fig. 4. Effect of pH on phenol removal by Den/TiO_2 ($C_{Adsorbent}$ = 0.3 g/L, C_0 = 20 mg/L, and T = 25°C).

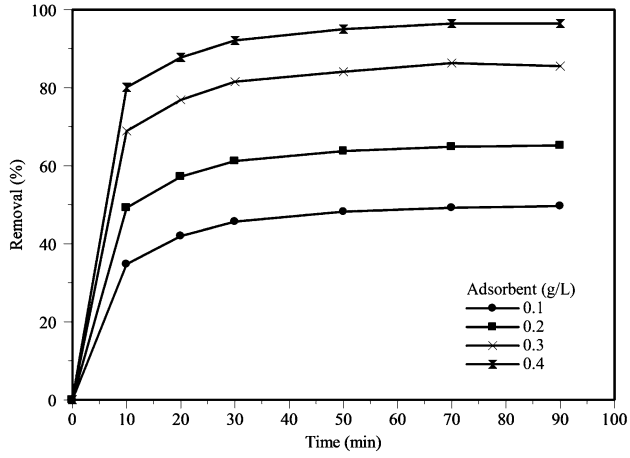

Fig. 5. Effect of adsorbent dosage on phenol removal using Den/TiO_2 (pH 7, C_0 = 20 mg/L, and T = 25°C).

Fig. 5, with the increase of adsorbent dosage, the removal efficiency steadily increases. The increase in adsorption with adsorbent dosage can be attributed to the higher adsorbent surface and the availability of more interior cavities to trap the phenol molecules. However, if the adsorption capacity was expressed in mg of phenol adsorbed per gram of Den/TiO_2, the adsorption capacity would decrease by increasing the adsorbent dosage. This may be due to the overlapping or aggregation of the adsorption sites resulting in a decrease in total adsorbent surface area available to phenol and increase in diffusion path length [27].

3.2.3. Effect of time

Fig. 5 also shows the removal of phenol as a function of contact time. Referring to this figure, the percentage of phenol removal is found to increase with increase in the contact time. In other words, contact time is used to assess the practical application of the adsorption process. It is observed that the removal of phenol by Den/TiO_2 is a slow process, where the adsorption takes place after 20 min and equilibrium is attained within 70 min. Beyond the equilibrium time, adsorption is found to be nearly constant. It can be explained that at the initial stage of the removal, unfilled cavities of Den/TiO_2 are available, and when the equilibrium is attained, the adsorption process will become slow, probably because of the repellent forces between the phenol molecules trapped in the Den/TiO_2 and the ones in the bulk solution [28].

3.2.4. Effect of temperature

The effect of temperature on adsorption process was investigated at four different temperatures (25, 35, 45, and 55°C) with phenol concentration of 20 mg/L. Fig. 6 exhibits the variation of phenol removal at these temperatures. The increase in temperature can affect the adsorption rate by altering the molecular interactions and the solubility. It may increase the mobility of phenol molecules and also produce a swelling effect within the internal structure of Den/TiO_2 to enable the phenol molecules to penetrate further through the structure of Den/TiO_2 [29–32].

3.2.5. Effect of initial phenol concentration

The influence of varying the initial phenol concentration (10, 20, 30, and 40 mg/L) was assessed on the removal efficiency, while the other parameters were kept constant at the previously obtained optimum values (Fig. 7). It is obvious that at the constant Den/TiO_2 dosage, the higher the initial phenol concentration, the lower the percentage of phenol removal. The resulted removal efficiency is acceptable (~85%) at phenol concentration of 20 mg/L, thus it was chosen as the optimum value for the phenol removal process [33].

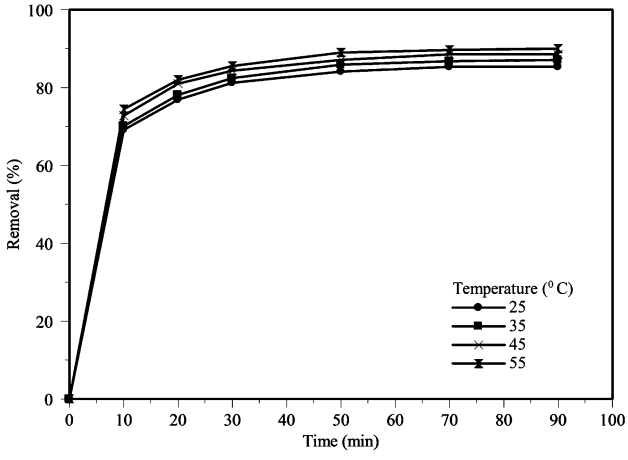

Fig. 6. Effect of temperature on phenol removal using Den/TiO_2 ($C_{Adsorbent}$ = 0.3 g/L, C_0 = 20 mg/L, and pH 7).

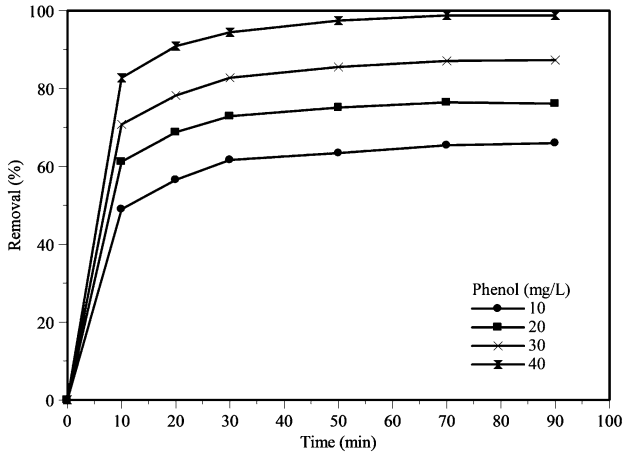

Fig. 7. Effect of initial phenol concentration on phenol removal by Den/TiO_2 ($C_{Adsorbent}$ = 0.3 g/L, T = 25°C, and pH 7).

3.3. Isotherms studies

In this study, two isotherm models (Langmuir and Freundlich) have been examined to describe the experimental data of the removal process to optimize the design of an adsorption system for the removal of phenol from solutions.

3.3.1. Langmuir isotherm

The Langmuir equation is often described by a monolayer adsorption. This model assumes a uniform energy of adsorption and a single layer of adsorbed solute at a constant temperature. The Langmuir model is the most frequently employed model and is given by Eq. (2) [34]:

$$q_e = Q_0 K_L C_e / (1 + K_L C_e) \quad (2)$$

where q_e, C_e, Q_0, and K_L are the amount of solute adsorbed at equilibrium (mg/g), the concentration of adsorbate at equilibrium (mg/L), maximum

adsorption capacity (mg/g), and Langmuir constant (L/mg), respectively. The linear form of the Langmuir equation is written as Eq. (3) [35]:

$$\frac{C_e}{q_e} = \frac{1}{K_L Q_0} + \frac{C_e}{Q_0} \tag{3}$$

To study the applicability of the Langmuir isotherm for the phenol encapsulation by Den/ TiO_2, linear plot of C_e/q_e against C_e is plotted and the values of Q_0, K_L, R_L, and R_1^2 (correlation coefficient) are shown in Table 2. The essential characteristics of the Langmuir isotherm can be expressed by a dimensionless constant called equilibrium parameter, R_L, which is defined by Eq. (4) [22]:

$$R_L = 1/(1 + K_L C_0) \tag{4}$$

The R_L values determine the nature of the adsorption process to be either unfavorable ($R_L > 1$), linear ($R_L = 1$), favorable ($0 < R_L < 1$), or irreversible ($R_L = 0$). The obtained values of R_L indicated that the removal process was favorable (Table 2) [36].

3.3.2. Freundlich isotherm

The Freundlich equation is another well-known model to investigate the adsorption process. It is an empirical equation to describe the distribution of solute between the solid and aqueous phase at the point of saturation. The basic assumption of this model is that there is an exponential variation in the site energies of the adsorbent and surface adsorption is not the rate limiting step [37]. The Freundlich isotherm is derived by assuming a heterogeneous surface with a non-uniform distribution of heat of adsorption over the surface. This isotherm can be expressed by Eq. (5) [30,38–40]:

$$q_e = K_F C_e^{1/n} \tag{5}$$

where K_F is the adsorption capacity at unit concentration and $1/n$ is the adsorption intensity. $1/n$ values indicate the type of isotherm to be irreversible ($1/n = 0$), favorable ($0 < 1/n < 1$), and unfavorable ($1/n > 1$) [41]. Eq. (5) can be rearranged to the linear form as Eq. (6):

$$\log q_e = \log K_F + 1/n \log C_e \tag{6}$$

The linear plot of log q_e vs. log C_e was plotted and the values of K_F, n, and R_2^2 (correlation coefficient) are also shown in Table 2. The results demonstrate that the removal of phenol from solution follows the Langmuir isotherm with high correlation coefficient values.

Table 2
Isotherm parameters for phenol removal by Den/TiO_2 ($C_{Adsorbent}$ = 0.3 g/L, C_0 = 20 mg/L, and pH 7)

Langmuir isotherm				Freundlich isotherm		
Q_0	K_L	R_L	R_1^2	K_F	$1/n$	R_2^2
77	1.869	0.001	0.996	48	0.111	0.993

3.4. Kinetic studies

In this study, pseudo-first-order and pseudo-second-order kinetic models have been used to test the obtained experimental data [42,43].

3.4.1. Pseudo-first-order kinetic

Pseudo-first-order equation is generally represented by Eq. (7) [44,45]:

$$dq_t/dt = k_1(q_e - q_t) \tag{7}$$

where k_1 is the equilibrium rate constant of pseudo-first-order kinetic model (1/min). After integration and applying the conditions ($q_t = 0$ at $t = 0$ and $q_t = q_t$ at $t = t$) Eq. (7) can be written as Eq. (8):

$$\log(q_e - q_t) = \log(q_e) - k_1/2.303t \tag{8}$$

The straight-line plots of log $(q_e - q_t)$ vs. t for the removal of phenol by Den/TiO_2 have been used to obtain the rate parameters. k_1, the experimental q_e, and correlation coefficients (R^2) at different phenol concentrations were calculated and given in Table 3.

3.4.2. Pseudo-second-order kinetic

The experimental data were applied to the pseudo-second-order kinetic model which is expressed by Eq. (9) [41,43]:

$$dq_t/dt = k_2(q_e - q_t) \tag{9}$$

where k_2 is the equilibrium rate constant of pseudo-second-order kinetic model (g/(mg min)). Integration of Eq. (9), will result the following equation:

$$t/q_t = 1/k_2 q_e^2 + (1/q_e)t \tag{10}$$

Table 3
Kinetic constants for pseudo-first- and pseudo-second-order model for phenol removal by Den/TiO_2 ($C_{Adsorbent}$ = 0.3 g/L, C_0 = 20 mg/L, and pH 7)

		Pseudo-first-order			Pseudo-second-order		
Phenol (mg/L)	$(q_e)_{Exp}$	$(q_e)_{Cal.}$	k_1	R^2	$(q_e)_{Cal.}$	k_2	R^2
10	100	58	0.074	0.927	103	0.003	0.999
20	170	113	0.071	0.956	178	0.001	0.999
30	216	147	0.069	0.954	227	0.001	0.999
40	228	181	0.066	0.976	243	0.001	0.999

The linear plots of t/q_t vs. t for the phenol removal were drawn, and the obtained k_2, experimental q_e, and correlation coefficients (R^2) are also given in Table 3.

The kinetic of phenol removal using Den/TiO_2 can be approximated as pseudo-second-order (Table 3) due to the high R^2 values [36]. The results (Fig. 8) indicate that the experimental q_e values agree with the calculated q_e obtained from the linear plots of pseudo-second-order kinetic model (Table 3).

3.5. Thermodynamic studies

Thermodynamic parameters including the Gibbs free energy (ΔG), enthalpy (ΔH), and entropy (ΔS) are the actual indicators for the practical application of an adsorption process. According to the values of these parameters, the spontaneous nature of the process can be determined. The thermodynamic parameters were determined using the Eqs. (11)–(13): [40]

$$\Delta G = \Delta H - T\Delta S \tag{11}$$

$$K_c = q_e/C_e \tag{12}$$

$$\ln K_c = \Delta S/R - \Delta H/RT \tag{13}$$

where K_c, q_e, C_e, R, and T are the equilibrium constant, the amount of phenol adsorbed on the adsorbent at equilibrium (mg/g), the equilibrium concentration of phenol in the solution (mol/L), the gas constant (8.314 J/mol K), and the absolute temperature (K), respectively. By plotting the graph of ln K_c vs. $1/T$, the values of ΔH and ΔS can be estimated from the slope and intercept, respectively (Fig. 9).

The obtained thermodynamic parameters are given in Table 4. Positive ΔH value suggests that the adsorption process is an endothermic reaction. On the other hand, positive value of ΔS indicates the increased randomness at the solid/solution interface during the encapsulation of phenol using Den/TiO_2. The negative values of ΔG imply the spontaneous nature of the removal process. Furthermore, the decrease in the values of ΔG by increasing the temperature indicates that

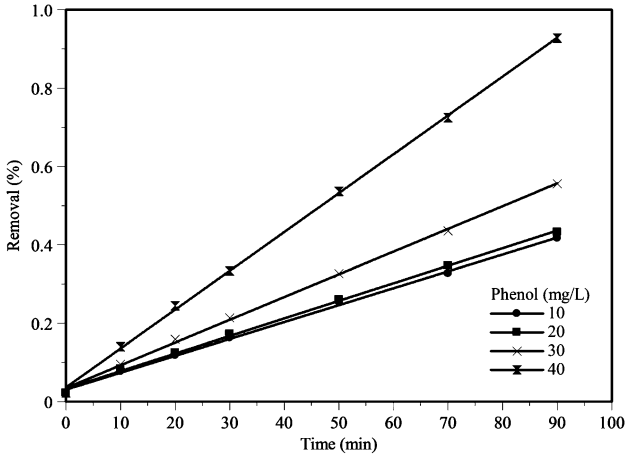

Fig. 8. Linear form of pseudo-second-order kinetic model for phenol removal using Den/TiO_2 ($C_{Adsorbent}$ = 0.3 g/L, T = 25°C, and pH 7).

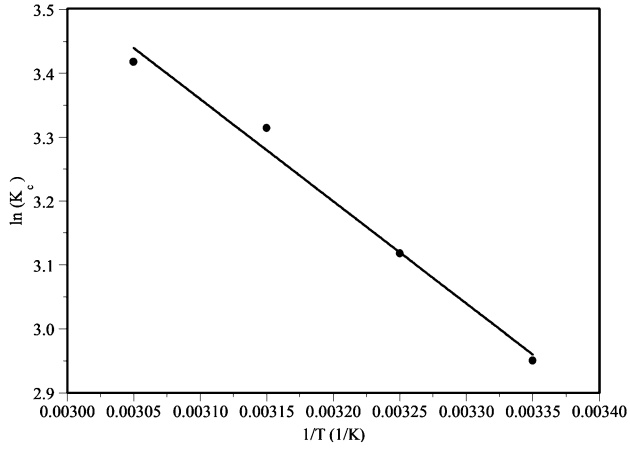

Fig. 9. Thermodynamic study for phenol removal using Den/TiO_2 ($C_{Adsorbent}$ = 0.3 g/L and pH 7).

Table 4
Thermodynamic parameters for phenol removal by Den/TiO_2 ($C_{Adsorbent}$ = 0.3 g/L, C_0 = 20 mg/L, and pH 7)

		ΔG (kJ/mol) at temperatures				
ΔH (kJ/mol)	ΔS (J/mol K)	298 K	308 K	318 K	328 K	338 K
12.843	67.564	−7.291	−7.966	−8.642	−9.317	−9.416

the removal process is more spontaneous at higher temperatures. In addition, the change in Gibbs free energy for physisorption is between −20 and 0 kJ/mol, but chemisorption is in the range of −80 to −400 kJ/mol [36,46]. The values of Δ*G* obtained in this study are within the ranges of the physisorption mechanism, which also confirms the physical entrapment of phenol molecules in the cavities of Den/TiO_2.

4. Conclusion

In this research, the preparation, characterization, and phenol encapsulation of a new biocompatible nanohybrid (Den/TiO_2) were investigated. Characterization of Den/TiO_2 was studied by FTIR, XRD, TEM, and SEM analysis, which demonstrated the successful synthesis of Den/TiO_2 and confirmed the effective surface area for the removal of phenol from aqueous solutions. TiO_2 nanoparticles played an important role to block the surface amino groups of the PAMAM dendrimer and to prohibit them from repelling the phenol molecules. The suggested mechanism for the removal of phenol (which was resulted from the ineffectiveness of pH on the removal efficiency) was the encapsulation of phenol molecules in the internal cavities of dendrimer and Van der Waals attraction between the benzene ring of phenol and alkane chains of PAMAM dendrimer. The effect of key parameters including pH, time, initial phenol concentration, Den/TiO_2 dosage, and temperature was investigated on removal efficiency, and the results demonstrated that the phenol removal by Den/TiO_2 was a rather slow process. The Langmuir and Freundlich isotherm models were investigated and the obtained data were best fitted to the Langmuir model with high correlation coefficient values. In addition, the kinetic data were well fitted to the pseudo-second-order model rather than the pseudo-first-order. The thermodynamic parameters indicated that the removal of phenol was an endothermic and spontaneous process. The overall obtained results showed that the novel Den/TiO_2 nanohybrid synthesized in this research can effectively remove phenol from aqueous solutions and improve the wastewater quality.

Acknowledgments

The present investigation was sponsored by INSF (www.insf.gov.org) under the project number "89001855", for which the authors wish to offer their gratitude to this organization for their support.

References

[1] I. Alinnor, M. Nwachukwu, Adsorption of phenol on surface—Modified cassava peel from its aqueous solution, Int. J. Environ. Sci. 1(2) (2012) 68–76.
[2] M. Kilic, E. Apaydin-Varol, A.E. Pütün, Adsorptive removal of phenol from aqueous solutions on activated carbon prepared from tobacco residues: Equilibrium, kinetics and thermodynamics, J. Hazard. Mater. 189(1–2) (2011) 397–403.
[3] M. Caetano, C. Valderrama, A. Farran, J.L. Cortina, Phenol removal from aqueous solution by adsorption and ion exchange mechanisms onto polymeric resins, J. Colloid Interface Sci. 338(2) (2009) 402–409.
[4] M. Carvalho, M. da Motta, M. Benachour, D. Sales, C. Abreu, Evaluation of BTEX and phenol removal from aqueous solution by multi-solute adsorption onto smectite organoclay, J. Hazard. Mater. 239–240 (2012) 95–101.
[5] L. Damjanović, V. Rakić, V. Rac, D. Stošić, A. Auroux, The investigation of phenol removal from aqueous solutions by zeolites as solid adsorbents, J. Hazard. Mater. 184(1–3) (2010) 477–484.
[6] J. Hu, M. Fang, Y. Cheng, J. Zhang, Q. Wu, T. Xu, Host−guest chemistry of dendrimer−drug complexes. 4. An in-depth look into the binding/encapsulation of guanosine monophosphate by dendrimers, J. Phys. Chem. B. 114(21) (2010) 7148–7157.
[7] J. Lim, G.M. Pavan, O. Annunziata, E.E. Simanek, Experimental and computational evidence for an inversion in guest capacity in high-generation triazine dendrimer hosts, J. Am. Chem. Soc. 134(4) (2012) 1942–1945.
[8] D. Astruc, E. Boisselier, Dendrimers designed for functions: From physical, photophysical, and supramolecular properties to applications in sensing, catalysis, molecular electronics, photonics, and nanomedicine, Chem. Rev. 110(4) (2010) 1857–1959.
[9] V.S. Myers, M.G. Weir, E.V. Carino, D.F. Yancey, S. Pande, R.M. Crooks, Dendrimer-encapsulated nanoparticles: New synthetic and characterization methods and catalytic applications, Chem. Sci. 2(9) (2011) 1632–1646.
[10] D. Yamamoto, T. Koshiyama, S. Watanabe, M.T. Miyahara, Synthesis and photoluminescence characterization of dendrimer-encapsulated CdS quantum dots, Colloids Surf., A 411 (2012) 12–17.

[11] M. Lard, S.H. Kim, S. Lin, P. Bhattacharya, P.C. Ke, M.H. Lamm, Fluorescence resonance energy transfer between phenanthrene and PAMAM dendrimers, Phys. Chem. Chem. Phys. 12(32) (2010) 9285–9291.
[12] W.-D. Jang, K. Kamruzzaman Selim, C.-H. Lee, I.-K. Kang, Bioinspired application of dendrimers: From bio-mimicry to biomedical applications, Prog. Polym. Sci. 34(1) (2009) 1–23.
[13] A.R. Menjoge, R.M. Kannan, D.A. Tomalia, Dendrimer-based drug and imaging conjugates: Design considerations for nanomedical applications, Drug Discovery Today 15(5–6) (2010) 171–185.
[14] K. Nwe, L.H. Bryant Jr., M.W. Brechbiel, Poly(amidoamine) dendrimer based MRI contrast agents exhibiting enhanced relaxivities derived via metal preligation techniques, Bioconjugate Chem. 21(6) (2010) 1014–1017.
[15] I. Asharani, D. Thirumalai, Synthesis of dendrimer-encapsulated silver nanoparticles and its catalytic activity on the reduction of 4-nitrophenol, J. Chin. Chem. Soc. 59(11) (2012) 1455–1460.
[16] C. Gutiérrez-Wing, J.J. Velázquez-Salazar, M. José-Yacamán, Procedures for the synthesis and capping of metal nanoparticles, in: Methods of Molecular Biology, vol. 906, Clifton, NJ, 2012, pp. 3–19.
[17] D.F. Yancey, E.V. Carino, R.M. Crooks, Electrochemical synthesis and electrocatalytic properties of Au@Pt dendrimer-encapsulated nanoparticles, J. Am. Chem. Soc. 132 (2010) 10988–10989.
[18] R. Li, A. Xie, W. Pang, Q. Zhu, K. Nie, Host–guest interaction and nano-microstructure of spherical poly(amidoamine) dendrimer/gold hybrid colloids under γ-ray irradiation, Mater. Lett. 67(1) (2012) 103–106.
[19] E. Murugan, G. Vimala, Synthesis, characterization, and catalytic activity for hybrids of multi-walled carbon nanotube and amphiphilic poly(propyleneimine) dendrimer immobilized with silver and palladium nanoparticle, J. Colloid Interface Sci. 396 (2013) 101–111.
[20] S. Sunoqrot, J. Bugno, D. Lantvit, J.E. Burdette, S. Hong, Prolonged blood circulation and enhanced tumor accumulation of folate-targeted dendrimer-polymer hybrid nanoparticles, J. Controlled Release 191 (2014) 115–122.
[21] M.A. Barakat, M.H. Ramadan, M.A. Alghamdi, S.S. Algarny, H.L. Woodcock, J.N. Kuhn, Remediation of Cu(II), Ni(II), and Cr(III) ions from simulated wastewater by dendrimer/titania composites, J. Environ. Manage. 117 (2013) 50–57.
[22] S. Akhtar, Q. Husain, Potential applications of immobilized bitter gourd (*Momordica charantia*) peroxidase in the removal of phenols from polluted water, Chemosphere 65(7) (2006) 1228–1235.
[23] C. Ng, J.N. Losso, W.E. Marshall, R.M. Rao, Freundlich adsorption isotherms of agricultural by-product-based powdered activated carbons in a geosmin–water system, Bioresour. Technol. 85(2) (2002) 131–135.
[24] C. Quintelas, E. Sousa, F. Silva, S. Neto, T. Tavares, Competitive biosorption of ortho-cresol, phenol, chlorophenol and chromium(VI) from aqueous solution by a bacterial biofilm supported on granular activated carbon, Process Biochem. 41(9) (2006) 2087–2091.
[25] E. Bustos, J. Manríquez, L. Echegoyen, L.A. Godínez, Preparation, characterization and photoelectrochemical study of mixed C60?Starburst® PAMAM G0.0 dendrimer films anchored on the surface of nanocrystalline TiO_2 semiconductor electrodes, Chem. Commun. 12 (2005) 1613–1615.
[26] M. Sadeghi-Kiakhani, M. Arami, K. Gharanjig, Dye removal from colored-textile wastewater using chitosan-PPI dendrimer hybrid as a biopolymer: Optimization, kinetic, and isotherm studies, J. Appl. Polym. Sci. 127(4) (2012) 2607–2619.
[27] H.B. Senturk, D. Ozdes, A. Gundogdu, C. Duran, M. Soylak, Removal of phenol from aqueous solutions by adsorption onto organomodified Tirebolu bentonite: Equilibrium, kinetic and thermodynamic study, J. Hazard. Mater. 172(1) (2009) 353–362.
[28] U.F. Alkaram, A.A. Mukhlis, A.H. Al-Dujaili, The removal of phenol from aqueous solutions by adsorption using surfactant-modified bentonite and kaolinite, J. Hazard. Mater. 169(1–3) (2009) 324–332.
[29] A. Szyguła, E. Guibal, M. Ruiz, A.M. Sastre, The removal of sulphonated azo-dyes by coagulation with chitosan, Colloids Surf., A 330(2–3) (2008) 219–226.
[30] F. Woodard, Industrial Waste Treatment Handbook, Butterworth-Heinemann, Burlington, MA, 2006.
[31] G. Annadurai, Design of optimum response surface experiments for adsorption of direct dye on chitosan, Bioprocess Biosyst. Eng. 23(5) (2000) 451–455.
[32] X.-W. Liu, X.-F. Sun, Y.-X. Huang, G.-P. Sheng, K. Zhou, R.J. Zeng, F. Dong, S.-G. Wang, A.-W. Xu, Z.-H. Tong, H.-Q. Yu, Nano-structured manganese oxide as a cathodic catalyst for enhanced oxygen reduction in a microbial fuel cell fed with a synthetic wastewater. Water Res. 44(18) (2010) 5298–5305.
[33] L. Eskandarian, E. Pajootan, M. Arami, Novel super adsorbent molecules, carbon nanotubes modified by dendrimer miniature structure, for the removal of trace organic dyes, Ind. Eng. Chem. Res. 53(38) (2014) 14841–14853.
[34] B. Subramanyam, D. Ashutosh, Adsorption isotherm modeling of phenol onto natural soils—Applicability of various isotherm models, Int. J. Environ. Res. 6(1) (2012) 265–276.
[35] S.K. Das, J. Bhowal, A.R. Das, A.K. Guha, Adsorption behavior of Rhodamine B on *Rhizopus oryzae* biomass, Langmuir 22(17) (2006) 7265–7272.
[36] L. Eskandarian, M. Arami, E. Pajootan, Evaluation of adsorption characteristics of multiwalled carbon nanotubes modified by a poly(propylene imine) dendrimer in single and multiple dye solutions: Isotherms, kinetics, and thermodynamics, J. Chem. Eng. Data 59(2) (2014) 444–454.
[37] K.K.H. Choy, J.F. Porter, G. Mckay, Intraparticle diffusion in single and multicomponent acid dye adsorption from wastewater onto carbon, Chem. Eng. J. 103 (1–3) (2004) 133–145.
[38] Q.Y. Cai, C.H. Mo, Q.T. Wu, Q.Y. Zeng, A. Katsoyiannis, J.F. Férard, Bioremediation of polycyclic aromatic hydrocarbons (PAHs)-contaminated sewage sludge by different composting processes, J. Hazard. Mater. 142(1–2) (2007) 535–542.
[39] N.M. Mahmoodi, Equilibrium, kinetics, and thermodynamics of dye removal using alginate in binary systems, J. Chem. Eng. Data 56(6) (2011) 2802–2811.

[40] N.M. Mahmoodi, B. Hayati, H. Bahrami, M. Arami, Dye adsorption and desorption properties of *Mentha pulegium* in single and binary systems, J. Appl. Polym. Sci. 122(3) (2011) 1489–1499.
[41] E.R.Alley, Water Quality Control Handbook, McGraw-Hill, New York, NY, 2007.
[42] A. Demirbas, Heavy metal adsorption onto agro-based waste materials: A review, J. Hazard. Mater. 157(2–3) (2008) 220–229.
[43] Y.S. Ho, G. McKay, The kinetics of sorption of divalent metal ions onto sphagnum moss peat, Water Res. 34(3) (2000) 735–742.
[44] A.A. Yawalkar, D.S. Bhatkhande, V.G. Pangarkar, A.A.C.M. Beenackers, Solar-assisted photochemical and photocatalytic degradation of phenol, J. Chem. Technol. Biotechnol. 76(4) (2001) 363–370.
[45] H. Yuh-Shan, Citation review of Lagergren kinetic rate equation on adsorption reactions, Scientometrics 59(1) (2004) 171–177.
[46] Ö. Gerçel, A. Özcan, A.S. Özcan, H.F. Gerçel, Preparation of activated carbon from a renewable bio-plant of *Euphorbia rigida* by H_2SO_4 activation and its adsorption behavior in aqueous solutions, Appl. Surf. Sci. 253(11) (2007) 4843–4852.